Bending energy of buckled edge dislocations

Raz Kupferman*
Einstein Institute of Mathematics, The Hebrew University, Jerusalem 91904, Israel
(Received 4 September 2017; published 11 December 2017)

The study of elastic membranes carrying topological defects has a longstanding history, going back at least to the 1950s. When allowed to buckle in three-dimensional space, membranes with defects can totally relieve their in-plane strain, remaining with a bending energy, whose rigidity modulus is small compared to the stretching modulus. In this paper we study membranes with a single edge dislocation. We prove that the minimum bending energy associated with strain-free configurations diverges logarithmically with the size of the system.

DOI: 10.1103/PhysRevE.96.063002

I. INTRODUCTION

The energetics of two-dimensional (2D) elastic membranes with defects has been studied extensively in the past several decades (e.g., [1,2]). In a crystalline setting, one may model a 2D solid with a single disclination by a triangular lattice perturbed by a unique vertex of degree either 5 (positive disclinations) or 7 (negative disclinations) [3]. Likewise, a 2D solid with a single dislocation can be modeled by a triangular lattice perturbed by a 5-7 pair. In a continuum setting, the geometry of the elastic membrane is modeled by a Riemannian metric describing local equilibrium distances between neighboring material elements. The ordered state is modeled by a Euclidean metric, implying that the membrane can be embedded locally in Euclidean plane without stretching. Defects are modeled by singularities in the metric [4]: A disclination corresponds to a Dirac measure–valued Gaussian curvature, whereas a dislocation corresponds to a dipole of Gaussian curvature. The presence of defects constitutes a metric incompatibility between the intrinsic geometry of the membrane and the planar geometry.

When confined to planar configurations, an elastic membrane with defects of either type will necessarily be metrically distorted. In a crystalline setting, distortions manifest as a stretching or a compression of lattice bonds; in a continuum setting, distortions manifest as deviations of the actual metric of the embedded membrane from its reference metric. The elastic energy of a configuration is a measure of this metric distortion. It is evidently model dependent; however, prototypical models assume an elastic energy that scales quadratically with the local distortion.

In this paper we focus on membranes with single dislocations. It is well known that the elastic (stretching) energy E_S of planar configurations is bounded from below by a term depending quadratically on the magnitude of the dislocation (the Burgers vector) and diverging logarithmically with both the linear size of the system R and the radius r_0 of a core region around the defect, which can be either removed from the model or regularized; this scaling is sharp, in the sense that an upper bound with the same scaling can be obtained for low-energy configurations.

If allowed, thin membranes can buckle in the 3D ambient space [1–3]. Buckling allows for the full relaxation of the stretching energy E_S; in geometric terms, this means that up to some finite core, a surface with a dislocation can be embedded in 3D Euclidean space isometrically. From an energetic point, stretching energy E_S is being traded for a bending energy E_B, which is a higher-order measure of distortion, where the relevant small parameter is typically the ratio of the membrane thickness t and the system size L; in certain cases, e.g., in graphene, an effective measure of plate thickness is defined by the ratio of bending and stretching moduli. The bending energy is related to the so-called Willmore functional, i.e., the surface integral of the membrane's mean curvature squared. There exists vast literature on the dimensional reduction of 3D elasticity into so-called plate, shell, and membrane models, starting from phenomenological arguments [5], through asymptotic analyses [6,7], and, more recently, rigorous limit theorems [8,9]; in the metrically incompatible context, an asymptotically based argument was presented in [10], followed by rigorous analyses in [11,12].

A question of both fundamental and practical importance (e.g., the melting transition in 2D membranes [2,13]) is whether low-energy configurations of buckled dislocations remain finite as R tends to infinity. A natural reference system is that of a disclination, which may also be embedded isometrically in 3D Euclidean space, however, with a bending energy diverging logarithmically with the R; see [14,15] for recent rigorous analyses departing from 3D models. Heuristic arguments have suggested that in dislocations, which are bound pairs of disclinations of opposite signs, the logarithmic contributions may cancel out, giving rise to an energy bound independent of R. Numerical simulations were performed in [3], supporting these heuristics.

It should be noted that there is a certain degree of fuzziness in the statement that low-energy configurations are independent of R. Starting either from a full 3D model or from a Koiter plate model [7],

$$E_{\text{total}} = E_S + t^2 E_B,$$

two distinct limits may be considered: the plate limit $t \to 0$ and the "thermodynamics" limit $R \to \infty$. It is not at all clear that these two limits are interchangeable. If t is taken to zero first for finite R and a removed core, theorems establish that the low-energy states are isometric immersions, i.e., states of zero stretching energy. After rescaling the energy by t^2, the leading-order energy is the bending energy, now

*raz@math.huji.ac.il

restricted to the space of isometric immersions. A key question is whether the minimal bending energy remains finite as $R \to \infty$. Alternatively, one may let $R \to \infty$ first for finite t. Assuming that finite-energy states exist (possibly combining both stretching and bending contributions), one could study the $t \to 0$ limit. A third alternative would be to let $t \to 0$ and $R \to \infty$ simultaneously, assuming a certain relation between both variables.

It is not clear to what extent these distinct alternatives have been recognized in the literature. Most references mention the fact that out-of-plane buckling allows for the complete elimination of stretching energy. It seems a common belief that the bending energy of strain-free buckled dislocations is either R independent or at least diverges with R slower than logarithmically.

We prove that this is not the case; we show that the bending energy can be bounded from below by a term diverging logarithmically with R, which is, in this sense, similar to a disclination (even though the two cases differ substantially, as will be discussed). Specifically, our main result is the following.

Theorem 1. Consider a 2D annulus of inner radius r_0 and outer radius R, endowed with a metric representing an edge dislocation with the Burgers vector b. Then the bending energy of isometric immersions of that surface into $\mathbb{R}^3$ is bounded from below by

$$E_B \geqslant \frac{b^2}{128\pi^3 r_0^2} \log \frac{R}{r_0}. \tag{1}$$

This result is somewhat surprising if one compares disclinations and dislocations from a dimensional perspective. Take a plane with a disclination of magnitude α and consider an annular slice of radius r and width Δr; a simple dimensional argument shows that when embedded isometrically in $\mathbb{R}^3$, its minimum bending energy scales like $(\alpha/r)\Delta r$ (see also Appendix E), hence the logarithmic divergence with the size of the system. A similar dimensional argument for a narrow annular slice of a dislocated plane yields a minimum bending energy of order $(b^2/r^3)\Delta r$ [see (9) below]; one would naively expect the bending energy to be size independent. A more subtle analysis is needed to show that the propagation of curvature in a locally Euclidean surface yields a bending energy that is logarithmically diverging with the size of the system.

II. GEOMETRY OF AN EDGE DISLOCATION

The geometry of a single edge dislocation can be defined independently of any parametrization [16,17]. The membrane is modeled as a 2D Riemannian manifold $(\mathcal{M},\mathfrak{g})$ having an annular topology. The metric $\mathfrak{g}$ is locally Euclidean: Every point $p \in \mathcal{M}$ has an open neighborhood isometrically embeddable in the Euclidean plane. A locally Euclidean geometry implies a flat (Levi-Cività) connection $\nabla^{\mathcal{M}}$ or, equivalently, a locally path-independent parallel transport. The difference between a disclination and a dislocation is that in the latter case, the net curvature "at the core of the annulus" is zero (trivial holonomy), namely, parallel transport is globally path independent. We denote the parallel transport by $\Pi_p^q : T_p\mathcal{M} \to T_q\mathcal{M}$ for $p,q, \in \mathcal{M}$. The presence of a dislocation is

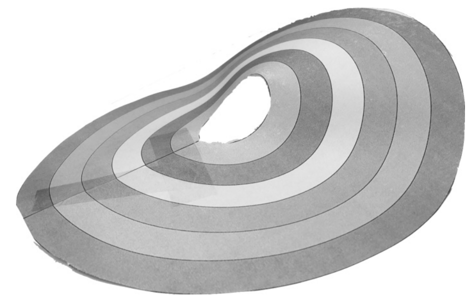

FIG. 1. Image of a buckled membrane with an edge dislocation.

additionally reflected by a nonzero circulation: There exists a $\nabla^{\mathcal{M}}$-parallel vector field $b \in \Gamma(T\mathcal{M})$ such that for every closed loop $\gamma : I \to \mathcal{M}$ encircling the core (homotopic to the inner boundary) and for every reference point $p \in \mathcal{M}$,

$$\int_I \Pi^p_{\gamma(t)}(\dot\gamma(t))dt = b_p,$$

where the evaluation of a vector field at a point is denoted by a subscript, as in b_p (this integral is the continuum counterpart of the lattice step counting in crystalline solids). Finally, the size of the system is imposed by setting the geodesic curvatures of the inner and outer boundaries to be close to r_0 and R, respectively. In edge dislocations, as opposed to screw dislocations, the magnitude of the Burgers vector cannot exceed the perimeter $2\pi r_0$ of the inner boundary.

While the geometry of an edge dislocation is well defined (up to immaterial details) by the above characterization, a coordinate representation is often more suitable for calculations. A convenient coordinate representation is the following. We use polarlike coordinates

$$(r,\varphi) \in [r_0,R] \times [0,2\pi),$$

where periodicity in φ is assumed. In these coordinates, the metric $\mathfrak{g}$ is given by

$$\mathfrak{g}(r,\varphi) = dr \otimes dr + [r_0 + (r - r_0)\kappa]^2 d\varphi \otimes d\varphi,$$

where $\kappa(\varphi) = 1 + B \cos\varphi$ and $|B| < 1/2$ is a dimensionless parameter related to the ratio of the Burgers vector and the core size. We note that the frame field $\{e_1,e_2\}$, with

$$e_1 = \partial_r, \quad e_2 = [r_0 + (r - r_0)\kappa]^{-1}\partial_\varphi,$$

is orthonormal. The geodesic curvature of constant-r curves is $k_g(\varphi) = \kappa(\varphi)/r$ and their perimeter is $2\pi r$. One may furthermore verify that the Gaussian curvature vanishes locally, i.e., the manifold is locally Euclidean, and that the holonomy is trivial. Finally, the Burgers vector equals $b = -2\pi r_0 J_1(B)e_2$, where J_1 is the Bessel function of the first kind (see Appendix A for details).

A configuration of $(\mathcal{M},\mathfrak{g})$ is an immersion $\mathbf{x} : \mathcal{M} \to \mathbb{R}^3$, where $\mathbb{R}^3$ is endowed with the standard Euclidean metric; an image of a configuration of an edge-dislocated paper sheet is shown in Fig. 1. Denoting by $H : \mathcal{M} \to \mathbb{R}$ the mean curvature of $\mathbf{x}(\mathcal{M})$ in $\mathbb{R}^3$, the bending energy associated with $\mathbf{x}$ is given by

$$E_B(\mathbf{x}) = \int_{\mathcal{M}} H^2 d\mathcal{V}_{\mathfrak{g}}, \tag{2}$$

where $d\mathcal{V}_\mathfrak{g}$ is the area element induced by $\mathfrak{g}$. Here we focus on membranes with effectively zero thickness, where only bending deformations are allowed. Therefore, our goal is to find a lower bound for E_B over all isometric immersions $\mathbf{x} : \mathcal{M} \to \mathbb{R}^3$.

III. PROOF OF THEOREM 1

In this section we derive the lower bound (1). First, there is an analytical subtlety that needs to be addressed: The functional (2) is naturally defined on the space of Sobolev functions $W^{2,2}(\mathcal{M};\mathbb{R}^3)$; correspondingly, derivatives should be interpreted in a weak sense. Hornung [18] (building upon the work of Pakzad [19]) proved that the set of smooth isometric immersions is dense in the $W^{2,2}$ topology within the set of $W^{2,2}$ isometric immersions. Thus, the infimum of E_B over smooth isometric immersions is the same as its infimum over $W^{2,2}$ isometric immersions. In other words, the bending energy for isometric immersions cannot be lowered by deteriorating the regularity. In practical terms, this implies that we may restrict our analysis to smooth maps.

We fix $r \in [r_0,R]$ and consider the constant-r curve in arc-length parametrization $\gamma : [0,2\pi r) \to \mathcal{M}$; clearly, $\dot{\gamma} = e_2$. By the definition of the Burgers vector,

$$\int_0^{2\pi r} \Pi_{\gamma(t)}^{\gamma(0)}(e_2)dt = b_{\gamma(0)}. \tag{3}$$

On the other hand, we denote by $\varpi_x^y : T_x\mathbb{R}^3 \to T_y\mathbb{R}^3$ the parallel transport in $\mathbb{R}^3$; since $\mathbb{R}^3$ is defect-free,

$$\int_0^{2\pi r} \varpi_{\mathbf{x}(\gamma(t))}^{\mathbf{x}(\gamma(0))}[d\mathbf{x}_{\gamma(t)}(e_2)]dt = 0. \tag{4}$$

Operating with $d\mathbf{x}_{\gamma(0)}$ on (3) and subtracting (4), we obtain

$$\int_0^{2\pi r} \mathcal{Q}(t)(e_2)dt = d\mathbf{x}_{\gamma(0)}(b_{\gamma(0)}), \tag{5}$$

where

$$\mathcal{Q}(t) = d\mathbf{x}_{\gamma(0)} \circ \Pi_{\gamma(t)}^{\gamma(0)} - \varpi_{\mathbf{x}(\gamma(t))}^{\mathbf{x}(\gamma(0))} \circ d\mathbf{x}_{\gamma(t)}.$$

Taking (Euclidean) norms in (5) and using the fact that $d\mathbf{x}$ is an isometry,

$$|b| \leqslant \int_0^{2\pi r} |\mathcal{Q}(t)|dt, \tag{6}$$

where the norm of $K(t) \in \mathrm{Hom}(T_{\gamma(t)}\mathcal{M}, T_{\mathbf{x}(\gamma(0))}\mathbb{R}^3)$ is induced by $\mathfrak{g}$ and the Euclidean metric; note that we write $|b|$ rather than $|b_{\gamma(0)}|$, since b is a parallel field, hence its norm is the same everywhere.

We proceed to estimate the integrand on the right-hand side of (6). Differentiating $|\mathcal{Q}(t)|^2$ with respect to t,

$$\frac{d|\mathcal{Q}|^2}{dt} = 2\sum_{i=1}^{2} (\mathcal{Q}(e_i), d\mathbf{x}_{\gamma(0)} \circ \Pi_{\gamma(t)}^{\gamma(0)} \circ \nabla_{e_2}^{\mathcal{M}}(e_i)) - 2\sum_{i=1}^{2} (\mathcal{Q}(e_i), \varpi_{\mathbf{x}(\gamma(t))}^{\mathbf{x}(\gamma(0))} \circ \mathbf{x}^*\nabla_{e_2}^{\mathbb{R}^3} \circ d\mathbf{x}_{\gamma(t)}(e_i)),$$

where $\mathbf{x}^*\nabla^{\mathbb{R}^3}$ is the pullback of the Euclidean connection. Substituting the definition of the second fundamental form of $\mathbf{x}(\mathcal{M})$ in $\mathbb{R}^3$,

$$\mathrm{II}(u,v) = \left(\mathbf{x}^*\nabla^{\mathbb{R}^3}\right)_u d\mathbf{x}(v) - d\mathbf{x}\left(\nabla_u^{\mathcal{M}} v\right), \quad u,v \in T\mathcal{M},$$

and the expression for the Cartan-Christoffel symbols [Eq. (A2)], we obtain after straightforward manipulations

$$\frac{d|\mathcal{Q}|^2}{dt} = 2\sum_{i=1}^{2} (\mathcal{Q}(e_i), \varpi_{\mathbf{x}(\gamma(t))}^{\mathbf{x}(\gamma(0))} \circ \mathrm{II}(e_2,e_i)).$$

Using the Cauchy-Schwarz inequality and the fact that ϖ_x^y is an isometry,

$$\frac{d}{dt}|\mathcal{Q}| \leqslant |\,\mathrm{II}\,|. \tag{7}$$

Since the surface is locally Euclidean, the norm of the second fundamental form coincides with the absolute mean curvature $|H|$. Furthermore, since $\mathcal{Q}(0) = 0$, it follows from (7) that

$$|\mathcal{Q}(t)| \leqslant \int_0^t |H(\gamma(s))|ds \leqslant \int_0^{2\pi r} |H(\gamma(s))|ds.$$

Substituting into (6),

$$\frac{|b|}{2\pi r} \leqslant \int_0^{2\pi r} |H(\gamma(s))|ds. \tag{8}$$

Squaring and applying once again the Cauchy-Schwarz inequality, we finally obtain

$$\frac{|b|^2}{8\pi^3 r^3} \leqslant \int_0^{2\pi r} H^2(\gamma(s))ds. \tag{9}$$

Equation (9) is a lower bound on the integral of the mean curvature square along a constant-r loop. Since the left-hand side decays like $1/r^3$, integration over r yields a lower bound for E_B independent of R; this situation is very different from in disclinations, where a similar analysis yields a left-hand side proportional to $1/r$ [see Eq. (E1)], hence a bending energy with lower bound diverging logarithmically with R. Note that the difference between the two cases could have been anticipated by a simple dimensional argument.

Nevertheless, it would be premature to infer that the bending energy can be bounded independently of R. We have only learned that a diverging lower bound cannot be obtained by segmenting the annulus into annular stripes and summing up energy bounds for each stripe.

We proceed to the second part of the analysis, which consists of relating the bending content of the inner boundary with the bending content of loops inside the body. We denote by $\mathbf{x}_0(s) \in \mathbb{R}^3$, $s \in [0,2\pi r_0)$, the configuration of the inner boundary in arc-length parametrization and by $\mathfrak{t}(s) = \mathbf{x}_0'(s)$ the unit tangent. As is well known (e.g., [20]), a locally flat surface in $\mathbb{R}^3$ is a developable surface: It can be partitioned into flat points (where $H = 0$) and nonflat points, the latter constituting an open set. Through every nonflat point passes a unique asymptotic line, a geodesic (in $\mathcal{M}$) which maps under $\mathbf{x}$ into a geodesic (in $\mathbb{R}^3$). Asymptotic lines do not intersect and do not terminate until hitting the boundary.

The immersion $\mathbf{x}$ induces a semigeodesic parametrization of an open submanifold $\mathcal{M}'$ of $\mathcal{M}$. Specifically, we let $\mathcal{A} \subset [0,2\pi)$ be the set of values s for which $\mathbf{x}_0(s)$ is a nonflat point and set $\mathcal{M}'$ to be the union of the asymptotic lines emanating from

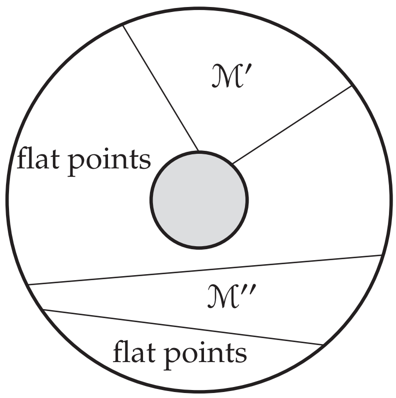

FIG. 2. Partition of $\mathcal{M}$ into flat and nonflat points. Here $\mathcal{M}'$ is the set of nonflat points connected by asymptotic lines to the inner boundary and $\mathcal{M}''$ is the set of nonflat points connected by asymptotic lines only to the outer boundary.

$\mathcal{A}$ (see Fig. 2). We parametrize $\mathcal{M}'$ with $s \in \mathcal{A}$ and with the arc length ρ along the asymptotic line; ρ ranges from 0 to some $\rho_{\max}(s)$ ranging between R and $R + r_0$ and depending on the angle between ∂_s and ∂_ρ. For every $s \in \mathcal{A}$ we let $\mathfrak{n}(s) \in \mathbb{R}^3$ be a unit vector along the embedded asymptotic line emanating through $\mathbf{x}_0(s)$. The restriction of $\mathbf{x}$ to $\mathcal{M}'$ is given, by construction, by

$$\mathbf{x}(\rho,s) = \mathbf{x}_0(s) + \rho\mathfrak{n}(s). \tag{10}$$

We proceed to claim that with no loss of generality, we may assume that $\mathcal{M}'$ contains *all* the nonflat points in $\mathcal{M}$. Indeed, consider, for example, the region marked $\mathcal{M}''$ in Fig. 2 and assume that it is a connected component of the set of nonflat points; as proved in [20], such a set, along with its boundary, is a union of $\mathcal{M}$ geodesics, mapped by $\mathbf{x}$ into straight lines. This region can be flattened without affecting the mean curvature in any other region, i.e., the bending energy can be reduced, without changing the restriction of $\mathbf{x}$ to $\mathcal{M}'$.

The metric induced by an immersion of the form (10) has entries

$$E = 1, \quad F = \mathfrak{t}\cdot\mathfrak{n}, \quad G = 1 + 2\rho\mathfrak{t}\cdot\mathfrak{n}' + \rho^2|\mathfrak{n}'|^2,$$

where we used the fact that $\mathfrak{n}\cdot\mathfrak{n}' = 0$ (see, e.g., [21] for a standard notation of the first and second fundamental forms). The unit vector $\mathfrak{n}$ cannot be chosen independently of $\mathbf{x}_0$; it follows from the Brioschi formula that the Gaussian curvature vanishes if and only if $\mathfrak{t}$, $\mathfrak{n}$, and $\mathfrak{n}'$ are coplanar (see Appendix B).

The second fundamental form of $\mathbf{x}(\mathcal{M}')$ in $\mathbb{R}^3$ is not an isometric invariant. By construction, the entries e and f of the second fundamental form vanish. The third entry g can be expressed as a function of ρ and the functions $\mathfrak{t}\cdot\mathfrak{n}$ and $\mathfrak{t}'\cdot\mathfrak{n}$ as a function of s; it follows directly from the Codazzi-Mainardi compatibility conditions (see [21], p. 111) that $g/\sqrt{EG-F^2}$ is independent of ρ, i.e., it is constant along asymptotic lines; expressing the mean curvature H in terms of the two fundamental forms, we obtain (see Appendix C) that

$$H\sqrt{EG-F^2} \quad \text{is independent of } \rho. \tag{11}$$

It remains to combine (11) together with the lower bound (8) to obtain a lower bound for the total bending energy. As shown in the Appendix D, a combination of the two yields the lower bound (1).

IV. DISCUSSION

We proved that the minimal bending energy of a strain-free buckled dislocation diverges logarithmically with the size of the system. This result may be surprising for two reasons: (i) The conjecture whereby the logarithmic divergence associated with two disclinations of opposite signs may cancel out turns out to be incorrect (ii) the scaling of the energy bound is the same as for disclinations. Note, however, the substantial difference between the two cases: For disclinations, the energetic contribution of a stripe at a distance r from the core scales like $O(1/r)$, whence the logarithmic divergence. For dislocations, the energetic contribution of a stripe scales like $O(1/r^3)$; the logarithmic divergence results from the propagation of curvature within the manifold. While the main focus here has been on the R dependence of the bending energy, note the substantial difference in the dependence on r_0: For disclinations, the bending energy of an isometric immersion is bounded from below by $C\log\frac{R}{r_0}$, where the dimensionless prefactor C depends on the magnitude of the disclination. Thus, increasing r_0 while retaining the defect intensity fixed has a mild effect in the case of a disclination, whereas for dislocations, the bending energy decreases quadratically with r_0. The distinction between disclinations and dislocations has a practical implication: If a cone is segmented into a set of narrow circular conical stripes, the total energy of all the segments when separated from each other is equal to the energy of the cone as a whole. This is not the case for a dislocation, where segmentation results in energetic relaxation.

Another interesting observation is the different scalings of bending and stretching energies in dislocations, assuming that the core radius r_0 and the Burgers vector b are of the same order. Then

$$E_S = 0 \Rightarrow t^2 E_B \sim t^2 \log\frac{R}{b},$$
$$E_B = 0 \Rightarrow E_S \sim b^2 \log\frac{R}{b}.$$

As to be expected, buckling is preferable only as long as the body is thin, i.e., t is smaller than all other intrinsic lengths.

As revealed in the Introduction, the order in which the limits $h \to 0$ and $R \to \infty$ are taken is substantial. The case where $t \to 0$ first and then $R \to \infty$ is well understood. A limiting behavior, which is not yet understood, is the case of finite thickness and infinite radius, letting then $t \to 0$. For such a case to make sense, one would first need to show that there exist configurations for which combined stretching and bending remain finite as $R \to \infty$. While the existence of such configurations is not doubted in the physics literature, a rigorous existence proof is still lacking.

ACKNOWLEDGMENTS

I am indebted to Michael Moshe for introducing me to this problem and for his invaluable advice. I have benefited from discussions with Cy Maor and from his critical reading of the manuscript. This research was partially funded by the Israel Science Foundation (Grant No. 661/13) and by a grant from the Ministry of Science, Technology and Space, Israel and the Russian Foundation for Basic Research, the Russian Federation.

APPENDIX A: CARTAN'S MOVING FRAMES FOR $(\mathcal{M},\mathfrak{g})$

The metric structure of $(\mathcal{M},\mathfrak{g})$ is conveniently analyzed using Cartan's formalism (see, e.g., [22], p. 359). We start by noting that the following frame field is orthonormal:

$$e_1 = \partial_r, \quad e_2 = [r_0 + (r - r_0)\kappa]^{-1}\partial_\varphi.$$

Its dual coframe is

$$\vartheta^1 = dr, \quad \vartheta^2 = [r_0 + (r - r_0)\kappa]d\varphi.$$

The Levi-Cività connection is defined by an antisymmetric family of 1-forms ω_α^β, where

$$\nabla_X e_\alpha = \omega_\alpha^\beta(X)\, e_\beta. \tag{A1}$$

In two dimensions, the connection is determined by a 1-form ω_2^1, satisfying Cartan's first structural equations

$$d\vartheta^1 + \omega_2^1 \wedge \vartheta^2 = 0, \quad d\vartheta^2 - \omega_2^1 \wedge \vartheta^1 = 0.$$

A straightforward calculation yields $\omega_2^1 = -dK$, where $K(\varphi) = \varphi + b\,\sin\varphi$. Since $d\omega_2^1 = 0$, it follows from Cartan's second structural equations that $(\mathcal{M},\mathfrak{g})$ is locally flat.

A direct substitution of the expression for ω_2^1 into (A1) yields the Cartan-Christoffel symbols

$$\nabla_{e_1}e_1 = 0, \quad \nabla_{e_1}e_2 = 0 \quad \nabla_{e_2}e_1 = \frac{\kappa}{r_0 + (r - r_0)\kappa}e_2,$$
$$\nabla_{e_2}e_2 = -\frac{\kappa}{r_0 + (r - r_0)\kappa}e_1, \tag{A2}$$

from which follows at once that $\nabla^{\mathcal{M}}$-parallel vector fields are spanned by the orthonormal frame field

$$\cos K e_1 + \sin K e_2, \quad -\sin K e_1 + \cos K e_2.$$

The fact that this frame is smooth across $\varphi = 0,2\pi$ implies the triviality of the holonomy.

Finally, to obtain the Burgers vector, consider the loop $\gamma(t) = (r_0,t)$ for $t \in [0,2\pi]$. Then

$$\dot\gamma(t) = \partial_\varphi = r_0 e_2.$$

Taking for a reference point $p = (r_0,0)$, we obtain that

$$\Pi^p_{\gamma(t)}(\dot\gamma(t)) = -r_0 \sin K(t)e_1|_p + r_0 \cos K(t)e_2|_p.$$

The Burgers vector at p is

$$\int_0^{2\pi} \Pi^p_{\gamma(t)}(\dot\gamma(t))dt = -r_0\int_0^{2\pi} \sin(t + B\sin t)dt\, e_1|_p + r_0\int_0^{2\pi} \cos(t + B\sin t)dt\, e_2|_p = -2\pi r_0 J_1(B)e_2|_p.$$

Since the Burgers vector is a parallel vector field [16], this equality is independent of the reference point p.

APPENDIX B: COMPATIBILITY CONDITIONS FOR EQ. (10)

Consider a surface of the form

$$\mathbf{x}(\rho,s) = \mathbf{x}_0(s) + \rho\mathfrak{n}(s) \tag{B1}$$

parametrized by the coordinate s taking values in some open set $\mathcal{A} \subset [0,2\pi)$ and the coordinate $\rho \in [0,\rho_{\max}(s)]$. Since

$$\frac{\partial f}{\partial\rho} = \mathfrak{n}, \quad \frac{\partial f}{\partial s} = \mathfrak{t} + r\mathfrak{n}', \tag{B2}$$

where $\mathfrak{t}(s) = \mathbf{x}_0'(s)$, it follows that the entries of the first fundamental form are

$$E = 1, \quad F = \mathfrak{t}\cdot\mathfrak{n}, \quad G = 1 + 2\rho\mathfrak{t}\cdot\mathfrak{n}' + \rho^2|\mathfrak{n}'|^2, \tag{B3}$$

where we used the fact that $\mathfrak{n}\cdot\mathfrak{n}' = 0$.

By the Brioschi formula (see [21], p. 112), the condition for the Gaussian curvature to vanish is

$$-\tfrac{1}{2}G_{\rho\rho}(EG - F^2) + \tfrac{1}{4}G_\rho^2 E = 0,$$

where we used the fact that E is constant and that F does not depend on ρ. Substituting (B3),

$$-|\mathfrak{n}'|^2[1 + 2\rho\mathfrak{t}\cdot\mathfrak{n}' + \rho^2|\mathfrak{n}'|^2 - (\mathfrak{t}\cdot\mathfrak{n})^2] + (\mathfrak{t}\cdot\mathfrak{n}')^2 + \rho^2|\mathfrak{n}'|^4 + 2\rho\mathfrak{t}\cdot\mathfrak{n}'|\mathfrak{n}'|^2 = 0,$$

which simplifies into

$$(\mathfrak{t}\cdot\mathfrak{n})^2 + \left(\mathfrak{t}\cdot\frac{\mathfrak{n}'}{|\mathfrak{n}'|}\right)^2 = 1. \tag{B4}$$

Since $\mathfrak{n}$ and $\mathfrak{n}'/|\mathfrak{n}|$ are orthonormal and since $\mathfrak{t}$ is a unit vector, (B4) implies that $\mathfrak{t}$ is coplanar with $\mathfrak{n}$ and $\mathfrak{n}'$.

APPENDIX C: DERIVATION OF EQ. (11)

Consider the surface (B1) satisfying the compatibility condition derived in the preceding appendix (i.e., $\mathfrak{t}$, $\mathfrak{n}$, and $\mathfrak{n}'$ are coplanar). We denote the entries of the second fundamental form by

$$e = \frac{\partial^2\mathbf{x}}{\partial\rho^2}\cdot\mathfrak{N}, \quad f = \frac{\partial^2\mathbf{x}}{\partial\rho\,\partial s}\cdot\mathfrak{N}, \quad g = \frac{\partial^2\mathbf{x}}{\partial s^2}\cdot\mathfrak{N},$$

where

$$\mathfrak{N} = \frac{\partial_\rho\mathbf{x}\times\partial_s\mathbf{x}}{|\partial_\rho\mathbf{x}\times\partial_s\mathbf{x}|}$$

is the unit normal to the surface. Substituting (B2),

$$\mathfrak{N} = \frac{\mathfrak{n}\times\mathfrak{t}}{|\mathfrak{n}\times\mathfrak{t}|}.$$

Since $\partial^2\mathbf{x}/\partial\rho^2 = 0$, it follows that $e = 0$. Likewise,

$$f = \mathfrak{n}'\cdot\frac{\mathfrak{n}\times\mathfrak{t}}{|\mathfrak{n}\times\mathfrak{t}|} = 0$$

because $\mathfrak{t}$, $\mathfrak{n}$, and $\mathfrak{n}'$ are coplanar. With that, the Codazzi-Mainardi compatibility conditions reduce to

$$\frac{\partial g}{\partial\rho} = g\Gamma_{12}^2,$$

where

$$\Gamma^2_{12} = \frac{-FE_s + EG_\rho}{2\det\mathcal{J}} = \frac{1}{2}\frac{\partial}{\partial\rho}\log(\det\mathcal{J}),$$

and we define

$$\det\mathcal{J} = EG - F^2 = 1 - (\mathfrak{t}\cdot\mathfrak{n})^2 + 2\rho\,\mathfrak{t}\cdot\mathfrak{n}' + \rho^2|\mathfrak{n}'|^2 = \frac{[1-(\mathfrak{t}\cdot\mathfrak{n})^2 - \rho\,(\mathfrak{t}'\cdot\mathfrak{n})]^2}{1-(\mathfrak{t}\cdot\mathfrak{n})^2}, \qquad \text{(C1)}$$

where in the last passage we used the fact that the collinearity of $\mathfrak{t}$, $\mathfrak{n}$, and $\mathfrak{n}'$ implies that $(\mathfrak{t}\cdot\mathfrak{n}')^2 = |\mathfrak{n}'|^2[1-(\mathfrak{t}\cdot\mathfrak{n})^2]$ and the fact that $\mathfrak{t}\cdot\mathfrak{n}' = -\mathfrak{t}'\cdot\mathfrak{n}$. It follows at once that

$$\frac{\partial}{\partial\rho}\frac{g}{\sqrt{\det\mathcal{J}}} = 0. \qquad \text{(C2)}$$

The mean curvature H is given by

$$H = \frac{1}{2\det\mathcal{J}}\mathrm{Tr}\left\{\begin{pmatrix} G & -F \\ -F & E\end{pmatrix}\begin{pmatrix} e & f \\ f & g\end{pmatrix}\right\} = \frac{Eg}{2\det\mathcal{J}},$$

which combined with (C2) implies that $H\sqrt{\det\mathcal{J}}$ is independent of ρ.

APPENDIX D: DERIVATION OF THE BOUND (1)

We start with Eq. (11), with the determinant of the first fundamental form given by (C1), and Eq. (8) for $r = r_0$,

$$\frac{|b|}{2\pi r_0} \leqslant \int_0^{2\pi r_0} |H(0,s)|ds. \qquad \text{(D1)}$$

The domain of integration on the right-hand side can be restricted to the set $\mathcal{A} \subset [0,2\pi r_0]$ corresponding to the nonflat points along the boundary.

We fix $\rho > 0$. Using the ρ invariance of $H\sqrt{\det\mathcal{J}}$,

$$\int_0^{2\pi r_0} |H(0,s)|ds = \int_0^{2\pi r_0} |H(0,s)|\frac{\sqrt{\det\mathcal{J}(0,s)}}{\sqrt{\det\mathcal{J}(0,s)}}ds = \int_0^{2\pi r_0} |H(\rho,s)|\sqrt[4]{\det\mathcal{J}(\rho,s)}\frac{\sqrt[4]{\det\mathcal{J}(\rho,s)}}{\sqrt{\det\mathcal{J}(0,s)}}ds.$$

Squaring, using the Cauchy-Schwarz inequality, and substituting (D1), we obtain

$$\frac{|b|^2}{4\pi^2 r_0^2} \leqslant \alpha(\rho)\int_0^{2\pi r_0} H^2(\rho,s)\sqrt{\det\mathcal{J}(\rho,s)}ds,$$

where

$$\alpha(\rho) = \int_0^{2\pi r_0}\frac{\sqrt{\det\mathcal{J}(\rho,s)}}{\det\mathcal{J}(0,s)}ds. \qquad \text{(D2)}$$

Integrating over ρ between zero and R,

$$E_B(\mathbf{x}) \geqslant \frac{|b|^2}{4\pi^2 r_0^2}\left(\int_0^R \frac{d\rho}{\alpha(\rho)}\right).$$

To obtain a logarithmic bound, it remains to bound $\alpha(\rho)$ from above by a term linear in ρ. It follows from (C1) that

$$\frac{\sqrt{\det\mathcal{J}(\rho,s)}}{\det\mathcal{J}(0,s)} = \frac{|1-(\mathfrak{t}\cdot\mathfrak{n})^2 - \rho\,(\mathfrak{t}'\cdot\mathfrak{n})|}{[1-(\mathfrak{t}\cdot\mathfrak{n})^2]^{3/2}}.$$

Thus, we need to bound $|\mathfrak{t}'\cdot\mathfrak{n}|$ from above and $1-(\mathfrak{t}\cdot\mathfrak{n})^2$ away from zero.

To bound the second, we consider a loop in the interior of the annulus. Rather than $(\rho,s) = (0,s)$ being an arc-length parametrization of the inner boundary $(r = r_0)$, we let $(0,s)$, $s \in [0,4\pi r_0)$, be a parametrization of the loop $r = 2r_0$. Thus, $\mathbf{x}_0(s)$ is the configuration of that loop, with $\mathfrak{t}(s)$ and $\mathfrak{n}(s)$ defined with respect to it. The analysis remains essentially unchanged, up to the fact that (i) Eq. (8) is evaluated at $r = 2r_0$, (ii) ρ ranges between $\rho_{\min}(s)$ and $\rho_{\max}(s)$, where $\rho_{\min}$ is between $(-2r_0)$ and $(-r_0)$ and $\rho_{\max}$ is between $R - r_0$ and R, and (iii) the upper integration limit in (D2) is $4\pi r_0$, resulting in a numerical prefactor

$$E_B(\mathbf{x}) \geqslant \frac{|b|^2}{16\pi^2 r_0^2}\left(\int_{-r_0}^{R-r_0}\frac{d\rho}{\alpha(\rho)}\right). \qquad \text{(D3)}$$

The key is that now $\mathfrak{t}(s)\cdot\mathfrak{n}(s)$ cannot be arbitrarily close to 1; otherwise the asymptotic line through $(0,s)$ will not intersect the inner boundary. Since $\mathbf{x} : \mathcal{M} \to \mathbb{R}^3$ is an isometric immersion,

$$\mathfrak{t}(s)\cdot\mathfrak{n}(s) = \mathfrak{g}_{(0,s)}(\partial_s,\partial_\rho),$$

i.e., the angle in $\mathbb{R}^3$ between $\mathfrak{t}(s)$ and $\mathfrak{n}(s)$ is equal to the angle in $\mathcal{M}$ between the s and ρ parametric lines at $(0,s)$. An elementary calculation shows that the angle between ∂_s and ∂_ρ is bounded from below by $\pi/3$, hence

$$1-(\mathfrak{t}\cdot\mathfrak{n})^2 \geqslant 1-\cos^2\frac{\pi}{3} = \frac{3}{4}.$$

Finally, $|\mathfrak{t}'\cdot\mathfrak{n}|$ is bounded by the geodesic curvature of $\mathbf{x}_0$, i.e., by $1/r_0$. It follows that

$$\alpha(\rho) \leqslant \int_0^{4\pi r_0}\frac{1+\rho/r_0}{1/2}ds = 8\pi(r_0+\rho).$$

Substituting into (D3), we finally obtain

$$E_B(\mathbf{x}) \geqslant \frac{|b|^2}{128\pi^3 r_0^2}\log\frac{R}{r_0}.$$

APPENDIX E: BENDING ENERGY OF A BUCKLED DISCLINATION

A lower bound for the bending energy of a buckled disclination can be obtained by an approach similar to that used for dislocations. A disclination can by parametrized using polarlike coordinates (r,φ) with the metric

$$\mathfrak{g}(r,\varphi) = dr\otimes dr + \alpha^2 r^2 d\varphi\otimes d\varphi.$$

Here $0 < \alpha < 1$ corresponds to a positive disclination and $\alpha > 1$ to a negative disclination. It is easy to see that

$$e_1 = \partial_r, \quad e_2 = \frac{1}{\alpha r}\partial_\varphi$$

is an orthonormal frame field. The dual coframe is

$$\vartheta^1 = dr, \quad \vartheta^2 = \alpha r d\varphi.$$

The solution of Cartan's first structural equations is

$$\omega^1_2 = -\alpha d\varphi.$$

The Cartan-Christoffel symbols are

$$\nabla_{e_1} e_1 = 0, \quad \nabla_{e_1} e_2 = 0, \quad \nabla_{e_2} e_1 = \frac{1}{r} e_2,$$
$$\nabla_{e_2} e_2 = -\frac{1}{r} e_1.$$

The perimeter of a constant-r loop is $2\pi\alpha r$.

Consider a vector $v \in T_{(r,0)}\mathcal{M}$ transported along the naturally parametrized constant-r curve

$$\gamma(t) = (r, t/\alpha r), \quad t \in [0, 2\pi\alpha r].$$

Then $\dot\gamma(t) = (e_2)_{\gamma(t)}$. Denoting by $(\Pi_\gamma)_0^t$ the parallel transport along γ, we obtain that

$$(\Pi_\gamma)_0^t(e_1) = \cos(t/r)e_1 - \sin(t/r)e_2,$$
$$(\Pi_\gamma)_0^t(e_2) = \sin(t/r)e_1 + \cos(t/r)e_2.$$

In particular, for $t = 2\pi\alpha r$,

$$(\Pi_\gamma)_0^{2\pi\alpha r}(e_1) = \cos(2\pi\alpha)e_1 - \sin(2\pi\alpha)e_2,$$
$$(\Pi_\gamma)_0^{2\pi\alpha r}(e_2) = \sin(2\pi\alpha)e_1 + \cos(2\pi\alpha)e_2.$$

On the other hand, we denote by $(\varpi_{\mathbf{x}\circ\gamma})_0^t$ the parallel transport operator in $\mathbb{R}^3$ along $\mathbf{x}\circ\gamma$. Clearly,

$$(\varpi_{\mathbf{x}\circ\gamma})_0^{2\pi\alpha r} = \mathrm{id}.$$

It follows that

$$\begin{aligned}\mathcal{Q}(v) &= [d\mathbf{x}_{\gamma(2\pi\alpha r)} \circ (\Pi_\gamma)_0^{2\pi\alpha r} - (\varpi_{\mathbf{x}\circ\gamma})_0^{2\pi\alpha r} \circ d\mathbf{x}_{\gamma(0)}](v)\\ &= [A(\alpha) - I] d\mathbf{x}_{\gamma(0)}(v),\end{aligned}$$

where $A(\alpha)$ is a rotation by an angle of $2\pi\alpha$. It follows that

$$|\mathcal{Q}| = |A(\alpha) - I|.$$

The evaluation of $|\mathcal{Q}|$ proceeds along the exact same line as for dislocations, yielding

$$|A(\alpha) - I| \leqslant \int_0^{2\pi\alpha r} |H(\gamma(t))| dt.$$

Squaring and using the Cauchy-Schwarz inequality, we finally obtain

$$\frac{|A(\alpha) - I|}{2\pi\alpha r} \leqslant \int_0^{2\pi\alpha r} H^2(\gamma(t)) dt. \tag{E1}$$

[1] J. Eshelby and A. Stroh, Dislocations in thin plates, Philos. Mag. **42**, 1401 (1951).

[2] D. Nelson and L. Peliti, Fluctuations in membranes with crystalline and hexatic order, J. Phys. **48**, 1085 (1987).

[3] H. S. Seung and D. R. Nelson, Defects in flexible membranes with crystalline order, Phys. Rev. A **38**, 1005 (1988).

[4] V. Volterra, Sur l'équilibre des corps élastiques multiplement connexes, Ann. Sci. Ecole Norm. Sup. Paris **24**, 401 (1907).

[5] T. von Kármán, Festigkeitsprobleme im maschinenbau, In *Encyclopädie der Mathematischen Wissenschafte*, edited by F. Klein and C. Mueller, Vol. 4 (1910), p. 311.

[6] A. Love, *A Treatise on the Mathematical Theory of Elasticity* (Cambridge University Press, Cambridge, 1927), fourth ed.

[7] W. Koiter, On the nonlinear theory of thin elastic shells, Proc. Kon. Ned. Acad. Wetensch. **69**, 1 (1966).

[8] H. Le Dret and A. Raoult, The nonlinear membrane model as a variational limit of nonlinear three-dimensional elasticity, J. Math. Pures Appl. **74**, 549 (1995).

[9] G. Friesecke, R. James, and S. Müller, A theorem on geometric rigidity and the derivation of nonlinear plate theory from three dimensional elasticity, Comm. Pure Appl. Math. **55**, 1461 (2002).

[10] E. Efrati, E. Sharon, and R. Kupferman, Elastic theory of unconstrained non-Euclidean plates, J. Mech. Phys. Solids **57**, 762 (2009).

[11] M. Lewicka and M. Pakzad, Scaling laws for non-Euclidean plates and the $W^{2,2}$ isometric immersions of Riemannian metrics, ESAIM: Control, Optimisation and Calculus of Variations **17**, 1158 (2010).

[12] R. Kupferman and J. Solomon, A Riemannian approach to reduced plate, shell, and rod theories, J. Func. Anal. **266**, 2989 (2014).

[13] D. Nelson, *Defects and Geometry in Condensed Matter Physics* (Cambridge University Press, Cambridge, 2002).

[14] H. Olbermann, Energy scaling law for a single disclination in a thin elastic sheet, Arch. Rat. Mech. Anal. **224**, 985 (2017).

[15] H. Olbermann (unpublished).

[16] R. Kupferman, M. Moshe, and J. Solomon, Metric description of defects in amorphous materials, Arch. Rat. Mech. Anal **216**, 1009 (2015).

[17] M. Moshe, I. Levin, H. Aharoni, R. Kupferman, and E. Sharon, Geometry and mechanics of two-dimensional defects in amorphous materials, Proc. Natl. Acad. Sci. USA **112**, 10873 (2015).

[18] P. Hornung, Approximating $W^{2,2}$ isometric immersions, C. R. Acad. Sci. Paris Ser. I **346**, 189 (2008).

[19] M. Pakzad, On the Sobolev space of isometric immersions, J. Diff. Geom. **66**, 47 (2004).

[20] W. Massey, Surfaces of Gaussian curvature zero in Euclidean space, Tohoku Math. J. **14**, 73 (1962).

[21] D. Struik, *Lectures on Classical Differential Geometry*, 2nd ed. (Dover, New York, 1961).

[22] C. Misner, K. Thorne, and J. Wheeler, *Gravitation* (Freeman, San Francisco, 1973).